

## **STRUCTURAL AND LUMINESCENCE PROPERTIES OF ALKALINE SUBSTITUTED LAMOX**

**Akhila Murali J<sup>1</sup>, K S Sibi\***

*\*,<sup>1</sup> Department of Physics, University of Kerala, Kariavattom Campus, Kerala-695581, India*

### **Abstract**

Lanthanum Molybdenum Oxide (LAMOX) has been identified as a potential entrant for Intermediate Temperature Solid Oxide Fuel Cell (IT- SOFC) applications. Here we are reporting the effect of Sodium substitution on the structural and luminescence properties of  $\text{La}_2\text{Mo}_2\text{O}_9$  prepared through solid state reaction route. In this paper, we focus on the structural studies of  $\text{Na}_x\text{La}_{2-x}\text{Mo}_2\text{O}_{9-x}$  (where  $x=0, 0.1, 0.2, 0.3, 0.4, 0.5, 0.6$ ) using XRD analysis and to optimize metastabilization of pure phase which shows intrinsic behaviors of LAMOX using DiffraC.suite 1.0 and TOPAS 4.2 analysis. Crystal Maker helps to visualize graphically the disordering and instabilities growing in the lattice at higher concentration. The UV – Vis response shows a band gap near to visible region and hence they have least probability to be an electronic conductor. The photoluminescence studies shows that the  $\text{La}_2\text{Mo}_2\text{O}_9$  does not show any luminescence effect due to the non-existence of f-f transition. But Na- substituted system behaves as a host for phosphor application with the emission peak near 624 nm.

**Keywords** LAMOX, Solid state reaction, XRD, Structure, Band gap, Emission spectrum

### **INTRODUCTION**

The electrolyte in SOFC feign for high temperature ionic conduction. To commence this as a socially and economically viable unit, SOFCs operating on low temperatures has to be developed. Conventionally developed solid oxide conductors belong to 4 major classes: fluorite type (stabilized zirconia [1], ceria,  $\delta$ -  $\text{Bi}_2\text{O}_3$  [2, 3]), deficient perovskites [4] (doped  $\text{LaGaO}_3$  [5, 6], brownmillerite phases), Aurivillius type phases (BIMEVOX) [7, 8] and Pyrochlores [9] ( $\text{Gd}_2\text{Zr}_2\text{O}_7$ ,  $\text{Gd}_2\text{Ti}_2\text{O}_7$ ) [10]. In 2000 Lacorre and his colleagues ratified that the LAMOX family which has been reported by Fournier et al. [11] in late 20s can act as fast oxide ionic conductors [12]. This LAMOX ionic conduction is noticeably voluminous than the ever reported best stabilized zirconia [13]. Like other ionic conductor [14, 15],

$\text{La}_2\text{Mo}_2\text{O}_9$  undergoes a phase transition from  $\alpha$ - monoclinic  $\text{La}_2\text{Mo}_2\text{O}_9$  to a high- temperature, more conducting cubic form ( $\beta$ -  $\text{La}_2\text{Mo}_2\text{O}_9$ ) [12]. A large number of substitutions are possible on the cationic and anionic sites of  $\text{La}_2\text{Mo}_2\text{O}_9$  thereby suppressing the phase transition and stabilizing the cubic phase at room temperature above a certain substitution [16- 18]. Various substitutions for both  $\text{La}^{3+}$  and  $\text{Mo}^{6+}$  were studied intensively for past few years [19-24]. Tealdi et al. reported the effect of alkaline- doping (Na, K, and Rb) on the properties of  $\text{La}_2\text{Mo}_2\text{O}_9$  and that was the first attempt to incorporate Na and Rb in the structure. Since the Na nucleus gives access to NMR Studies on a cationic site it is used as a possible Lanthanum substitution [25]. A. Selmi et al. [25] attempted to prepare Na substituted LAMOX samples through solid state reaction, but resulted

in impure cubic phases and hence did not extend the studies on lower Na contents. Hence the present study aims to analyze the effect of Na substitution in LAMOX in detail.

## EXPERIMENTAL

$\text{Na}_x\text{La}_{2-x}\text{Mo}_2\text{O}_9$  ( $x=0.0, 0.1, 0.2, 0.3, 0.4, 0.5, 0.6$ ) samples were prepared through conventional solid state reaction of stoichiometric mixture of  $\text{La}_2\text{O}_3$ ,  $\text{MoO}_3$  and  $\text{Na}_2\text{CO}_3$ . The thermal treatment was carried out in an alumina crucible, first at 500 °C for 12 hours to avoid Molybdenum Oxide melting and then at 1000 °C for 8 hours. Several regrinding and heating were necessary to obtain high purity phases. The room temperature X- ray diffraction data were recorded with Ni filtered Cu –  $\text{K}\alpha_1$  radiation using Bruker AXS D8 Advance Diffractometer in the  $2\theta$  range of 10- 80° with a step size of 0.0305°. The diffuse reflectance spectra of the prepared samples were recorded using Cary 5000 (2.23 version) UV- VIS NIR Spectrometer in the 200- 850 nm range of wavelength.  $\text{BaSO}_4$  is used as the reference material. The emission spectra of the calcined samples were studied for specific excitation wavelength using a Horiba Yvox Fluoromax 4 Spectrofluorometer with a 450 W Xenon flash lamp as the exciting source.

## RESULTS AND DISCUSSION

### XRD Analysis

Goutenoire et al. studied the structural properties of  $\alpha$ -  $\text{La}_2\text{Mo}_2\text{O}_9$  using both high-

resolution X- ray and neutron diffraction [17]. They reported that,  $\alpha$ -  $\text{La}_2\text{Mo}_2\text{O}_9$  has a lower symmetry than the  $\beta$ -  $\text{La}_2\text{Mo}_2\text{O}_9$  and the extra peaks present both in the X-ray and neutron diffraction patterns indicate the existence of a superstructure relative to  $\beta$ -  $\text{La}_2\text{Mo}_2\text{O}_9$ . Since the differences in the XRD patterns of the two phases are minima, we refer to the theoretical cubic phase in the following discussion.

The room temperature diffraction pattern of the pure compound is shown in Figure 1. It is in good agreement with the previously reported XRD pattern of  $\beta$ -  $\text{La}_2\text{Mo}_2\text{O}_9$  with the ICDD pattern no: 00-061-510, which has a  $\text{P}2_13$  (198) space structure and exhibits a cubic crystal structure. The high crystallinity is evident from the sharp diffraction peaks observed in X-ray diffraction pattern [26-29]. Tealdi et al. reported that there is some monoclinic distortion presented in the  $\beta$ - form. This distortion results in the presence of a few peaks with low intensity and in the splitting of some pseudo- cubic reflections corresponding to the cubic (111), (201), (211) and (321) reflections [30]. There are some side peaks near (211) and (410) (labeled with \*) can be noticed, which derive from the splits of the cubic reflection (211) and (410) [31] respectively. There are some additional peaks (labeled with #) present in the X-ray diffraction pattern near 17.53° and 37.86°. The X-ray powder diffraction pattern of the Na- substituted compounds in the  $2\theta$  range 10-80° is shown in Figure 2.

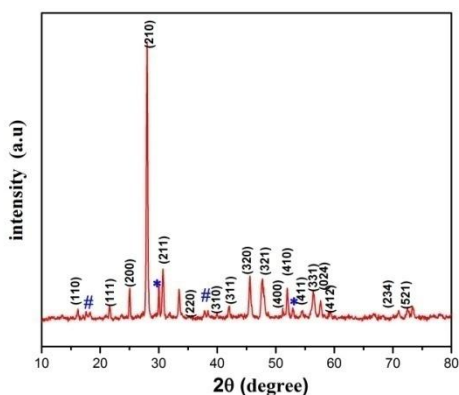


**Figure 1** X-ray diffraction pattern of  $\beta$ - $\text{La}_2\text{Mo}_2\text{O}_9$ , calcined at  $1000^\circ\text{C}$ .

An interesting observation was that the intensity of the splits in reflection (211) and (410), systematically diminished on going from  $x=0.1$  to  $x=0.6$ . Also the tiny diffraction peaks in Figure 1 disappear in the diffraction pattern of  $\text{Na}_x\text{La}_{2-x}\text{Mo}_2\text{O}_{9-\delta}$  system. This implies that the host is stabilized in cubic symmetry as the Na-substitution increases despite the existence of a small percentage of  $\alpha$ - $\text{La}_2\text{Mo}_2\text{O}_9$  [30]. The predominant diffraction peak corresponding to reflection (210), near  $27.86^\circ$  for the pure  $\text{La}_2\text{Mo}_2\text{O}_9$ , shows slight shift towards both lower and higher diffraction angle in the  $\text{Na}_x\text{La}_{2-x}\text{Mo}_2\text{O}_{9-\delta}$  system. It is because in the same coordinate surroundings the ionic radius for  $\text{Na}^+$  (1.02) and  $\text{La}^{3+}$  (1.03) is almost same [27, 32].

The diffraction pattern for the high temperature  $\text{Na}_x\text{La}_{2-x}\text{Mo}_2\text{O}_{9-\delta}$  system is refined considering a cubic structure in the  $P2_13$  (no. 198) space group, without taking into account the monoclinic distortion.

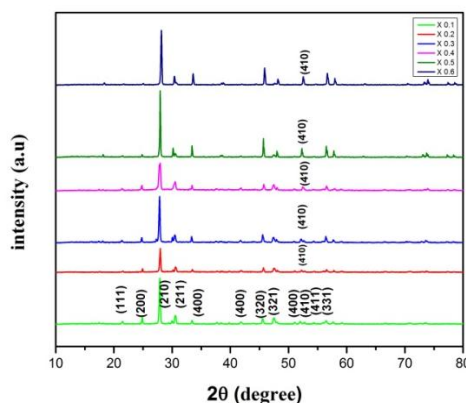


**Figure 2**  
**X-R-ray**

diffraction pattern of  $\text{Na}_x\text{La}_{2-x}\text{Mo}_2\text{O}_{9-\delta}$  ( $x=0.1, 0.2, 0.3, 0.4, 0.5, 0.6$ ) samples.

It should be noticed that the atomic positions and occupancies for Na- substituted system are similar to those reported for  $\beta$ - $\text{La}_2\text{Mo}_2\text{O}_9$ . To understand the structural variation the z- coordinate of O3 site atom is refined. Crystal Maker Software is employed to visualize the z- parameter variation of O3 site occupancy using  $\beta$ - cubic structure. O3 site migration and reordering of the oxygen channels are visualized for different samples are given in Figure 3. From the structures generated, oxygen ion exchange channel could be rationally visualized when viewed through (410) plane.

The lattice cell variation the x content is presented in the Table1. For  $\text{Na}^+$  substitution, the cell parameter decreases with increase in the dopant content. Also a contraction of the cell volume was observed which can be attributed to defect association of dopant and oxygen vacancies [33].

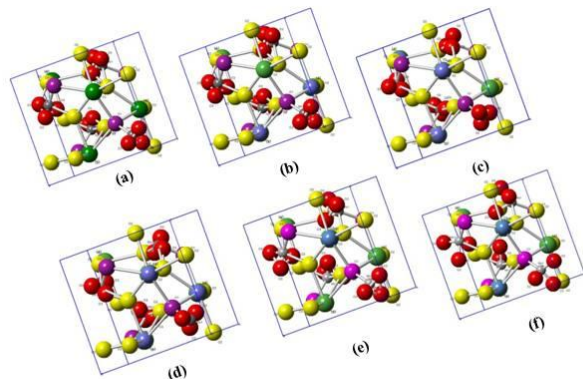


Figure 3 Structure generated for  $\text{Na}_x\text{La}_{2-x}\text{Mo}_2\text{O}_{9-\delta}$  ( $x=0.1, 0.2, 0.3, 0.4, 0.5, 0.6$ ) system viewed from (410) plane using Crystal Maker software.

Table 1 Lattice parameter

X content	Lattice parameter (Å)
0.0	7.13(3)
0.1	7.13(1)
0.2	7.13(1)
0.3	7.06(5)
0.4	7.01(9)
0.5	7.00(6)
0.6	6.95(9)

**UV- Vis Diffuse Reflectance Response**

The data plotted using Kubelka-Munk function is shown in Figure 4 with  $h\nu$  (eV) along X axis and  $[F(R_{\infty})/h\nu]^2$  along Y axis. It can be noted that on increasing the Na content, the optical absorption shows marked changes in its band gap. The band gap is near to visible region and hence they have least probability to be electronic conductors.

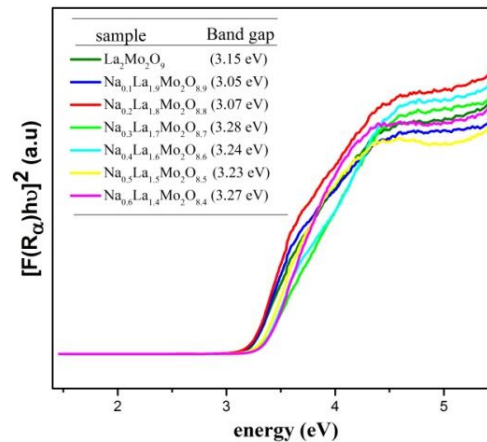


Figure 4 Kubelka- Munk Plot.

When  $x > 0.3$  in  $\text{Na}_x\text{La}_{2-x}\text{Mo}_2\text{O}_{9-\delta}$  system, band gap is almost invariant suggesting that Na substitution had not occurred in the lattice and the interaction between Na and La is more likely to be a minor phenomenon as inferred from XRD analysis.

**Photoluminescence Spectroscopy**

The photoluminescence of all samples prepared at 1000 °C was measured and their spectra are quite similar. Figure 5 plots the emission spectra of  $\text{Na}_x\text{La}_{2-x}\text{Mo}_2\text{O}_{9-\delta}$  samples. The Na- substituted samples shows an emission peak near 624 nm with relatively low intensity up to  $x = 0.4$ . It may be due to the fact that the Na-substitutions results in the creation of oxide ion vacancies in the lattice. So LAMOX can be used as potential candidate as host lattice in phosphor applications [34].

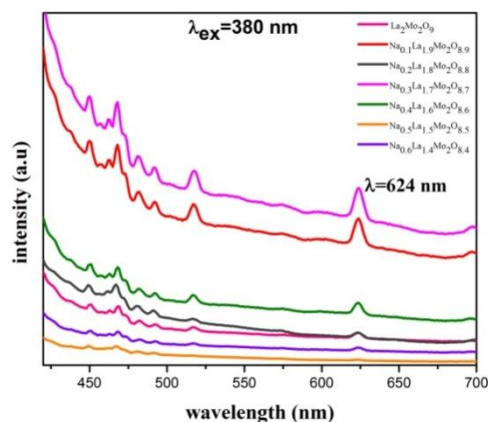


Figure 5 PL spectra of  $\text{Na}_x\text{La}_{2-x}\text{Mo}_2\text{O}_{9-\delta}$  ( $x=0.1, 0.2, 0.3, 0.4, 0.5,$  and  $0.6$ ) samples.

## CONCLUSIONS

In the present study, we have focused on effects of Sodium substitution in LAMOX family of oxides through solid state reaction route. The XRD studies carried out using Diffrac.suite 1.0, TOPAS 4.2 and Crystal Maker on Sodium substituted LAMOX helps us to visualize the reason for oxide ion conduction with proper theoretically refined structures. XRD analysis reveals that Sodium substitution in A site of  $\text{A}_2\text{B}_2\text{O}_9$  type LAMOX were stabilized in cubic structure and it envisage intrinsic oxide ion conduction by disordering O3 site parameters. Further a decrease in lattice parameter was observed with Na content. UV-Vis response reveals that band gap is near to visible region and hence they have least probability of being electronic conductors. The Na substituted samples shows an emission peak near 624 nm due to the creation of oxide ion vacancies in the lattice with Na substitution.

## REFERENCES

[1] E. C. Subbarao, Zirconia: an overview in Advances in Ceramics, eds. A. H. Heuer and L. W. Hobbs, vol. 3,

Science and Technology of Zirconia I, American Ceramic Society, Columbus, OH, (1981) 1-24.

- [2] T. Takahashi and H. Iwara, J. Appl. Electrochem., 3, (1973)65.
- [3] H. A. Harwig and A. G. Gerards, J. Solid State Chem., 26, (1978)265.
- [4] K. R. Kendall, C. Navas, J. K. Thomas and H.-C. zur Loye, Solid State Ionics, 82, (1995)215.
- [5] T. Ishihara, H. Matsuda and Y. Takita, J. Am. Chem. Soc., 116,(1994) 3801.
- [6] M. Feng and J. B. Goodenough, Eur. J. Solid State Inorg. Chem. 31 (1994) 663.
- [7] F. Abraham, M. F. Debreuille-Gresse, G. Mairesse and G. Nowogrocki, Solid State Ionics, 529 (1998) 28-30.
- [8] F. Abraham, J. C. Boivin, G. Mairesse and G. Nowogrocki, Solid State Ionics, 934 (1990) 40- 41.
- [9] H. L. Tuller, Solid State Ionics, 94 (1997)63.
- [10] S. A. Kramer and H. L. Tuller, Solid State Ionics. 82 (1995) 15.
- [11] Fournier, J. P., Fournier, J. & Kohlmuller, Bull. Soc. Chim. Fr. (1970) 4277- 4283.
- [12] Philippe Lacorre, Françoise Goutenoire, Odile Bohnke, Richard Retoux & Yvon Laligant, Nature, 404 (2000) 856-858.
- [13] S. Georges, F. Goutenoire, O. Bohnke, M. C. Steil, S. J. Skinner, H. D. Wiemhofer and P. Lacorre, J. New. Mat. Electrochem. Systems, 7(2004) 51-57.
- [14] Lacorre, P. & Retoux, R. J. Solid State Chem. 132 (1997) 443-446.
- [15] Boivin, J. C. & Mairesse, G. Chem. Mater. 10 (1998)2870-2888.
- [16] Kendall, K. R., Navas, C., Thomas, J. K. & zur Loye, H.-C. Solid State Ionics 82 (1995) 215- 223.
- [17] F. Goutenoire, O. Isnard, R. Retoux, and P. Lacorre, Chem. Mater., 12, (2000)2575-2580.
- [18] Sheldrick, G. M. Phase annealing in SHELX-90: direct methods for larger structures. Acta Crystallogr. A 46 (1990) 467- 473.

- [19] Jeitschko, W. & Sleight, A.W. Synthesis, properties and crystal structure of b-SnWO<sub>4</sub>. *Acta Crystallogr. B* 28 (1972) 3174 -3178.
- [20] Wells, A. F. *Structural Inorganic Chemistry* 5th edn, 1187 (Oxford Univ. Press, New York, 1987).
- [21] J. Galy, G. Meuneir, S. Andersson, A. Astrom, J. *Solid State Chem.*13 (1975) 142.
- [22] L. Baque, J. Vega-Castillo, S. Georges, A. Canerio, E. Djurado, *Ionics* 19 (2013) 1761.
- [23] P. Lacorre, A. Selmi, G. Corbel, B. Boulard, *Inorg. Chem.* 45 (2006) 627.
- [24] D. S. Tsai, M.J. Hsieh, J.C. Tseng, H.Y. Lee, J. *Eur. Ceram. Soc.*, 25(4) (2005) 481.
- [25] C. Tealdi, L. Malavasi, C. Ritter, G. Flor, G. Costa, J. *Solid State Chem.*, 181 (2008) 603-610.
- [26] Heremans C, Wuensch B J, Stalick J K and Prince E, J. *Solid State Chem.*117 (1995) 108.
- [27] R D Shannon, *Acta Cryst.* 32(1976) 751-767.
- [28] Nikiforov G, *Sov. Phys. Crystallgr.*17 (1972) 347.
- [29] Mc Cauly R A, J. *Appl. Phys.* 51 (1980) 290.
- [30] Cristina Tealdi, Gaetano Chiodelli, Lorenzo Malavasi and Giorgio Flor, *J. Mater. Chem.* 14 (2004) 3553-3557.
- [31] Dandan Zhang, ShikaoShi, MingLuo, JiZhou, *Ceramics International*, 39 (2013) 6299–6302.
- [32] J David Van Horn, *Electronuc Table of Shannon Ionic Radii*, (2001).
- [33] T. He, Y. Huang, Q. He, Y. Ji, L. Pei, Liu, Z. Lu, J. *Alloys Compd.* 388 (2005) 145.
- [34] [www. knetchemistry. com/links/Atomic Structure/ Waveenergy. Htm.](http://www.knetchemistry.com/links/Atomic%20Structure/Waveenergy.Htm)